

Increased confinement improvement in a reversed-field pinch using double-pulsed poloidal current drive

Y. Yagi,^{a)} H. Koguchi, Y. Hirano, T. Shimada, H. Sakakita, and S. Sekine
National Institute of Advanced Industrial Science and Technology (AIST), 1-1-1 Umezono, Tsukuba, Ibaraki 305-8568, Japan

B. E. Chapman and J. S. Sarff
University of Wisconsin, Madison, Wisconsin 53706

(Received 12 December 2002; accepted 18 April 2003)

The pulsed poloidal current drive (PPCD) [J. S. Sarff *et al.*, Phys. Rev. Lett. **72**, 3670 (1994)] experiment is conducted in a reversed-field pinch device, the toroidal pinch experiment RX (TPE-RX) after providing an auxiliary power supply system with increased energy in the main power supply system for the PPCD. The PPCD system thus provides double-pulsed operation with higher current in the toroidal coil than that in single-pulsed PPCD operation in TPE-RX [Y. Yagi *et al.*, Plasma Phys. Controlled Fusion **44**, 335 (2002)]. The central electron temperature, ion temperature, and electron density increase during PPCD, and there is, on average, a fivefold improvement in energy confinement, τ_E , relative to standard discharges. Double-pulsed PPCD yields better performance than that of single-pulsed PPCD operation where twofold improvement in τ_E was obtained. It is shown that the enhancement factor of τ_E in the double-pulsed PPCD experiment in TPE-RX is consistent with the trends, observed previously, versus magnetic fluctuation amplitude and versus $\Delta\gamma$, where $\Delta\gamma$ is the difference in $\gamma [= (1-F)/\Theta]$ between the start and the end of the PPCD period. © 2003 American Institute of Physics.
 [DOI: 10.1063/1.1581883]

I. INTRODUCTION

The reversed-field pinch (RFP)¹ is one of the systems for magnetically confining a thermonuclear fusion plasma. The RFP configuration is characterized by comparable B_p and B_t , where B_p and B_t are poloidal and toroidal magnetic fields, respectively, and by the reversal of B_t beyond $r/a \sim 0.8$, where a is the minor radius of the plasma. This magnetic configuration provides a relatively strong magnetic shear, which can sustain high plasma pressure. The RFP configuration can be sustained as long as the toroidal plasma current, I_p , is driven. The poloidal component of the plasma current is driven by the dynamo electric field² caused mainly by the fluctuating components in the $\mathbf{v} \times \mathbf{b}$ term in Ohm's law stemming from tearing instability. The tearing instability thus contributes to the sustainment of the RFP configuration, but, on the other hand, causes rapid global transport. This is the conventional picture of the RFP plasma.

Recently, experiments on current profile modification have been conducted in RFP plasmas, in order to stabilize the tearing instabilities and improve confinement. Pulsed poloidal current drive (PPCD) is one of the methods of current profile modification, which was originally conducted in the Madison Symmetric Torus, MST.³ PPCD is a technique for driving poloidal current inductively by ramping the current in the toroidal magnetic field coils. The idea underlying PPCD is to replace the dynamo electric field by applying a poloidal electric field, E_θ . Since the first experiment in

MST,³ PPCD performance has been improved step-by-step in MST,^{4,5} and the most recent experiment,⁵ using the five-pulsed PPCD with a reversed toroidal electric field, has achieved a tenfold improvement of the energy confinement time, τ_E , of 10 ms. PPCD was also applied in the reversed-field experiment, RFX.⁶ This allowed a twofold improvement in τ_E , with the observation of a reduction of electron energy transport in the core plasma.

In the toroidal pinch experiment, RX TPE-RX⁷ ($R/a = 1.72/0.45$ m), we also conducted the PPCD experiment, and obtained twofold improvement of τ_E .⁸ This PPCD experiment in TPE-RX was conducted using a toroidal reversal bank system. Recently, we increased the energy of the power supply for the toroidal reversal bank from its original 20 kJ to 170 kJ. We also installed additional toroidal coils with a new power supply system. Thus, a double-pulsed PPCD operation has now become possible. The double-pulsed PPCD has a longer pulse duration with more primary current in the toroidal coil to drive the poloidal current in the plasma. We report here the results of the double-pulsed PPCD experiment in TPE-RX.

It is observed in PPCD experiments in various RFP devices that magnetic and electron density fluctuations decrease at the edge as well as in the core region.^{3-6,8-10} It has been shown⁸ that the enhancement factor of τ_E in the previous PPCD experiments^{3-6,8} is inversely proportional to δb ,² where δb is the PPCD magnetic fluctuation amplitude normalized to that without PPCD. The reversal parameter, $F (= B_{ta}/\langle B_t \rangle)$, B_{ta} is the toroidal magnetic field at the plasma surface, and $\langle B_t \rangle$ is the volume averaged toroidal

^{a)}Electronic mail: y.yagi@aist.go.jp

field) is lowered, and the pinch parameter, Θ ($=B_{pa}/\langle B_t \rangle$, B_{pa} is the poloidal magnetic field on the plasma surface) increases. The RFP configuration is greatly but transiently changed during PPCD. It is shown that the enhancement factor of τ_E increases linearly with $\Delta\gamma$,¹¹ where $\Delta\gamma$ is the difference in γ [$= (1-F)/\Theta$] at the start and the end of PPCD. We show that the present work is consistent with the trend of the enhancement factor of τ_E versus δb^2 and $\Delta\gamma$.

The scope of the paper is as follows. The operating conditions and waveforms of the fundamental parameters in the PPCD and two kinds of standard discharge are described in Sec. II. Comparisons of the global confinement properties and magnetic fluctuation amplitudes between PPCD and standard discharges are shown in Secs. III and IV, respectively. The discussion and conclusion are given in Secs. V and VI.

II. PPCD AND STANDARD DISCHARGES

PPCD is conducted by driving current in the toroidal field windings to increase transiently the toroidal magnetic field reversal. Repetitions of transiently increasing B_{ta} can be applied to achieve a long PPCD period. The double-pulsed PPCD experiment in TPE-RX, hereafter called PPCD, is conducted using the auxiliary toroidal field system and the main toroidal reversal bank system in TPE-RX. The auxiliary toroidal field system consists of 16 evenly spaced coils of 4 turns each. Each coil has an independent power supply which has a 15.8 kJ capacitor bank of 100 V maximum working voltage. All 16 of the power supplies are simultaneously triggered in the PPCD experiment. Then the main toroidal reversal bank is triggered to superimpose the current in the 32 main toroidal coils (one turn each, connected in series). The trigger timing for the two power supplies is adjusted so that the soft-x-ray signal, I_{sx} , statistically becomes as large as possible. Before triggering the first PPCD pulse, toroidal reversal is maintained by the image current in the vacuum vessel, reacting to the increase of the toroidal flux during the current-rising phase of 20 ms. Therefore, the first PPCD pulse must be triggered before the image current decays, i.e., before F becomes zero, at around $t=20$ ms. From the previous work in MST,⁵ it is known that a key factor in operating PPCD is keeping the polarity of $E_{||}$ in the direction that drives the plasma current to sustain the RFP configuration, where $E_{||}$ is the parallel electric field on the plasma surface. We have also confirmed the importance of maintaining positive $E_{||}$ in PPCD in TPE-RX. Namely, maintaining positive $E_{||}$ in PPCD is necessary in order to avoid severe relaxation events which deteriorate confinement. Thus, we have optimized the trigger timing at $t=17$ and 21 ms for first and second PPCD pulse. It is shown below that the improvement due to PPCD lasts until $t=27$ ms, on average, and the smaller improvement follows until $t=33$ ms in the post PPCD phase. We have conducted PPCD experiments at $I_p=250, 300, 350,$ and 400 kA, and found that the best performance in terms of I_{sx} was obtained at $I_p=350$ kA. In this paper, we present the result obtained at $I_p=350$ kA with a deuterium fill pressure of 0.3–0.4 mTorr, which is the lowest possible startup pressure in TPE-RX. The equilibrium is

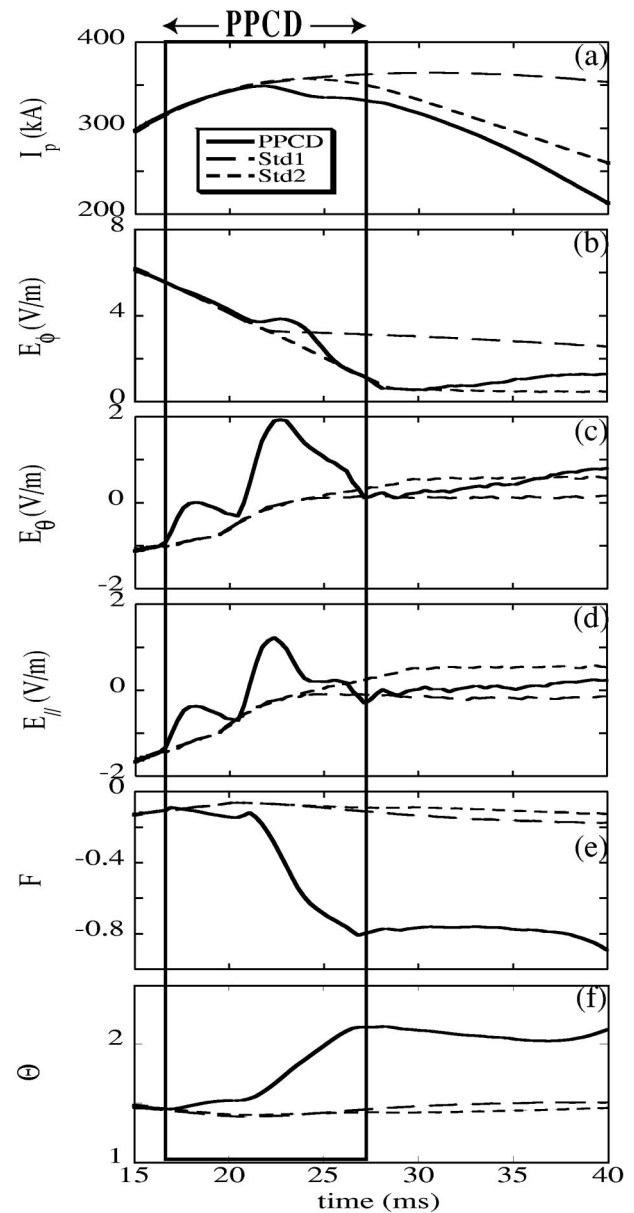


FIG. 1. Shot-averaged waveforms of the toroidal plasma current, I_p (a), toroidal electric field, E_ϕ (b), poloidal electric field, E_θ (c), parallel electric field, $E_{||}$ (d), reversal parameter, F (e) and pinch parameter, Θ (f) for PPCD (solid line), Std1 (long-dashed line) and Std2 (dashed line) plasmas.

maintained by the conductive shell system, and the error field at the thick shell gap is feedback controlled.

We compare three types of plasma. The first utilizes PPCD, and the other two are standard discharges without PPCD. In PPCD, we switch off the poloidal flat-top (I_p sustainment) bank in order to help sustain $E_{||}$ at the right polarity.⁵ One of the standard cases (Std1) utilizes the poloidal flat-top bank while the other (Std2) does not (like the PPCD plasmas). We present the two standard cases in order to clarify the effect of the I_p waveform. We conducted 66 PPCD discharges and 39 Std1 and 38 Std2 discharges.

Figure 1 shows the shot-averaged waveforms of the three plasma types. Figure 1(a) shows that I_p has a rounded waveform in PPCD and Std2 and that I_p in PPCD is slightly less than that in Std2, while I_p is sustained and the discharge

duration is longest, up to 80 ms, in Std1, which reflects the difference in the operation of the poloidal flat-top bank. The difference is directly seen in the toroidal electric field, E_ϕ , in Fig. 1(b). After $t=20$ ms, E_ϕ in Std1 decays more slowly than before $t=20$ ms, while E_ϕ decreases to 0.6 V/m in PPCD and Std2 at $t=30$ ms. The poloidal electric field, E_θ [Fig. 1(c)] shows double pulses corresponding to the PPCD operation. The largest value of 2 V/m is obtained at the peak of the second pulse.

A key controlling parameter of the PPCD operation is $E_{||}$. Figure 1(d) shows a comparison of $E_{||}$, which is negative and increasing during the current-rising phase in Std1 and Std2. The double pulses in the positive direction are seen in Fig. 1(d), which correspond to the PPCD operation. It is seen that $E_{||}>0$ is maintained for $t=21$ –27 ms. We note here that the first PPCD pulse is not large enough to make $E_{||}$ positive, but that the second pulse indeed produces positive $E_{||}$. However, we show in Sec. II that the effect of the first pulse is still finite as seen in I_{sx} , which indicates that the less negative $E_{||}$ in the first pulse can increase I_{sx} . We also note that $E_{||}$ in Std2 is positive and larger than that in Std1 at $t>24$ ms. This reflects the fact that E_ϕ acts to hinder the field-aligned current outside the reversal surface. This is the reason why E_ϕ should be as low as possible or should even be negative⁵ in PPCD to sustain positive $E_{||}$. It should be noted, however, that a quantitative positive correlation is not observed between the value of positive $E_{||}$ and the improvement factor of τ_E .

The RFP configuration, in terms of F and Θ , changes in time in PPCD. Figures 1(e) and 1(f) show waveforms of F and Θ , respectively. With each PPCD pulse, F is made more negative as a direct consequence of the negatively driven B_{ta} , and Θ increases accordingly. Note that F becomes as low as -0.8 and Θ becomes as high as 2.2 in PPCD. On the other hand, it should be noted here that F and Θ do not differ very much between Std1 and Std2, in spite of the differences in I_p , $\langle B_t \rangle$, and B_{ta} .

III. GLOBAL CONFINEMENT PROPERTIES

Shot-averaged I_{sx} and global confinement properties are compared among PPCD, Std1 and Std2 from 15 to 40 ms.

Figure 2(a) shows I_{sx} for the three cases. Note that I_{sx} , obtained by a Be-filtered surface barrier diode, is a function of electron density, n_e , and temperature, T_e . In PPCD, I_{sx} starts to increase after the first PPCD pulse at $t=17$ ms, shows a further increase after the second pulse at $t=21$ ms, and sharply rises after $t=25$ ms. The maximum I_{sx} is obtained at $t=27$ ms just before $E_{||}$ crosses zero and becomes negative again [Fig. 1(d)]. The maximum value of I_{sx} is one order of magnitude larger than that of Std1 and Std2. A slow decay of I_{sx} is observed after PPCD, and I_{sx} approaches the level in Std2 at $t\sim 40$ ms. In 18% of the PPCD plasmas, I_{sx} does not increase above Std cases. We note that the magnetic fluctuation amplitude is relatively large in these discharges, and these discharges were not included in Figs. 1 and 2. Note that the rest of the PPCD discharges (62%) are reproducible, but the standard deviation in the level of I_{sx} in PPCD increased in comparison with that in Std1 and Std2. The ex-

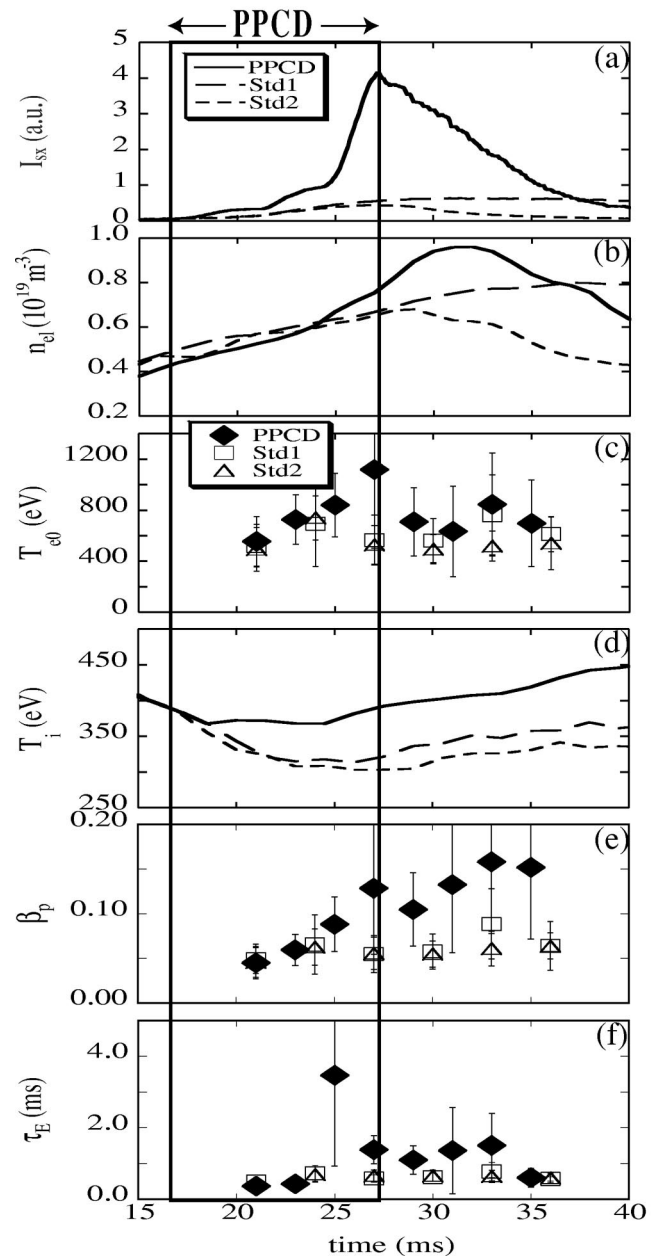


FIG. 2. Shot-averaged waveforms and data of the soft-x-ray signal, I_{sx} (a), line-averaged electron density, n_{el} (b), central electron temperature, T_{e0} (c), ion temperature, T_i (d), poloidal beta, β_p (e), and energy confinement time, τ_E (f) for PPCD (solid line, diamond), Std1 (long-dashed line, square) and Std2 (dashed line, triangle) plasmas.

perimental conditions to obtain good PPCD discharges are described in the recent PPCD experiment in MST.¹² It should also be noted that the effect of the decaying current and ohmic heating power in Std2 on I_{sx} appears after $t>25$ ms when the decay of I_p starts [Fig. 1(a)]. The soft-x-ray signal is sustained up to $t\sim 40$ ms in Std1 as long as I_p is sustained.

The line-averaged electron density, n_{el} , obtained using a two-color, heterodyne CO_2 interferometer, is shown in Fig. 2(b). The line-averaged electron density, n_{el} is comparable in the three cases before $t<24$ ms. Then n_{el} increases in PPCD, reaching a maximum of $1 \times 10^{19} \text{ m}^{-3}$ at $t=32$ ms after the end of the PPCD period. The PPCD increment of n_{el} at $t=27$

ms from those of Std1 and Std2 is 14%. It is also seen in Fig. 2(b) that n_{ei} decays as I_p decays in Std2, while n_{ei} gradually increases almost in proportion to I_p in Std1. The increment of n_{ei} in PPCD from that in Std2 is larger than the standard deviation. External fuelling was the same in the three cases, and the D_α line intensity decreases during the PPCD.⁸ Therefore, the increase n_{ei} is plausibly due to the reduced transport of electrons. Note that the D_α line intensity of Std1 after $t > 28$ ms is larger than that in Std2, and that the apparently larger n_{ei} in Std1 than that in Std2 in Fig. 2(b) does not indicate that the particle confinement in Std1 is higher than that in Std2.

The central electron temperature, T_{e0} , is measured using a single-pulse, single-point Thomson scattering system. We measured T_{e0} at eight time points in PPCD and six time points in Std1 and Std2. Between six and nine measurements were made at each time point. Figure 2(c) shows the shot-averaged T_{e0} for the three cases. It is seen in Fig. 2(c) that T_{e0} in PPCD has a peak at $t = 27$ ms when I_{sx} has a peak, and then drops to a level comparable to that in Std1 and Std2. The maximum value of $T_{e0} \sim 1$ keV is obtained at the peak, the value of which is a factor of two larger than in Std1 and Std2. The level of T_{e0} in Std1 confirms the previously reported result for Std1.¹³ Relatively large standard deviation accompanies each average value of T_{e0} , in comparison with those in n_{ei} and T_i , mainly because of the spatially and temporally pointwise nature of the Thomson scattering system and because of the relatively poor photon statistics. Somewhat larger error bars in PPCD than those in Std1 and Std2 reflect that the shot-by-shot deviation of the plasma performance in PPCD is larger than that in Std1 and Std2. It should be noted, however, that the hypothesis that T_{e0} in PPCD is higher than that in Std1 and Std2 is correct with a level of significance of 84%, because the difference of T_{e0} between PPCD and Std cases is comparable to the standard deviation of the distribution of T_{e0} in PPCD.

The ion temperature, T_i , is measured using an electrostatic neutral particle energy analyzer (NPA). Figure 2(d) shows that T_i in PPCD is slightly higher than in Std1 and Std2 after $t = 18$ ms, and the increment lasts well after the end of PPCD. The difference of T_i between PPCD and Std1/Std2 is approximately 100 eV, which is a difference outside the experimental error. This increase of T_i was also observed with single-pulse PPCD in TPE-RX,⁸ although the increment was smaller than in the present case. On the other hand, T_i did not change during the PPCD operation in MST.⁵ Since the equi-partition time from electrons to ions is on the order of 0.2 s,¹³ the ion heating mechanism in the standard RFP plasma is mainly attributed to magnetohydrodynamic (MHD) activity.¹⁴ The magnetic field fluctuation amplitude of the core-resonant $m=1$ modes, where m is the poloidal mode number, decreases in PPCD, while that of the edge-resonant $m=0$ modes in PPCD remains comparable to or somewhat larger than that of the Std cases, as described in Sec. IV. The reason why T_i increases in PPCD is unclear. The increase of T_i during the PPCD period may be an indication of reduced ion energy transport.

We calculate the poloidal beta, $\beta_p [= \langle p \rangle / (B_{pa}^2 / 2\mu_0)]$, where $\langle p \rangle$ is the volume averaged plasma pressure, μ_0 is the

vacuum permeability] assuming fixed spatial profiles, $T_e(r)/T_{e0} = T_i(r)/T_{i0} = n_e(r)/n_{e0} = [1 - (r/a)^3]$ and $n_i = n_e$, where the subscript “0” indicates a central value, $T_{i0} = T_i$ (NPA) is assumed, and n_i is the ion density. The volume-averaged plasma pressure, $\langle p \rangle$, is calculated from $\langle n_e(r) [T_e(r) + T_i(r)] \rangle$. Note that $\langle p \rangle$ is only weakly affected by the power of (r/a) in the profile function. For example, $\langle p \rangle$ is larger by 25% when $1 - (r/a)^6$ is assumed than when $1 - (r/a)^3$ is assumed. The β_p calculated for the three cases is plotted in Fig. 2(e), which shows that β_p increases after $t > 24$ ms in PPCD, and has a local peak at $t = 27$ ms. β_p still increases later on and has a higher peak at around $t = 33$ ms. The large β_p value after the PPCD period results from the fact that $\langle p \rangle$, particularly n_e and T_i , is sustained during the strong decay of I_p , in the post-PPCD period. The peak value of β_p at $t = 27$ ms is approximately 13%, which is approximately twice as high as β_p in Std1 and Std2. Note that the total beta, $\beta_{tot} = \langle p \rangle / [(B_{pa}^2 + B_{ta}^2) / 2\mu_0] = 11\%$ at $t = 27$ ms, which is also twice as high as β_{tot} in Std1 and Std2.

The estimation of $\tau_E [= W_s / (P_{Oh} - dW_s/dt)]$ in PPCD requires a proper treatment of the Ohmic input power, $P_{Oh} (= R_p I_p^2)$ and the rate of change of the stored thermal energy, $W_s (= 3\pi^2 R a^2 \langle p \rangle)$, since these values vary in time, and dW_s/dt can be comparable to P_{Oh} . In the present work, P_{Oh} is calculated after subtracting the inductive term in the loop voltage using the α - Θ model.¹⁵ The time derivative of W_s is calculated after temporally smoothing the discrete measurement of T_{e0} , n_{ei} , and T_i . The τ_E obtained in PPCD has a sharp peak at $t = 25$ ms and a broad plateau for $t = 27$ – 33 ms as shown in Fig. 2(f). The shot-averaged peak value of τ_E at $t = 25$ ms is 3.5 ms which is a factor of five larger than in Std1 and Std2. The peak has a large standard deviation mainly due to the large deviation of the denominator, $P_{Oh} - dW_s/dt$, in the definition of τ_E . From the statistical point of view, however, as discussed for the increment of T_{e0} , in PPCD, the hypothesis that PPCD yields higher τ_E than the average τ_E in the Std cases is correct with a level of significance of approximately 84%. Note that at $t = 25$ ms P_{Oh} has a minimum of 3 MW, and dW_s/dt has a maximum of 1.4 MW, so that $P_{Oh} - dW_s/dt$ is minimum then. The rate of change of $P_{Oh} - dW_s/dt$ exceeds that of W_s which has a peak at $t = 27$ ms. Thus the peak of τ_E appears at a time different from that when I_{sx} and β_p peak. Note that the input power from the capacitor banks of PPCD is mainly consumed in order to increase the magnetic energy of the plasma, which increases with Θ [Fig. 1(f)]. The transient nature of PPCD makes the estimation of $P_{Oh} - dW_s/dt$ difficult. However, as in early PPCD experiments in MST,^{3,4} we believe that we have reliably estimated P_{Oh} using the conventional α - Θ model under the assumption of fixed profile shape, but not magnitude for $T_e(r)$, $T_i(r)$, and $n_e(r)$.

IV. MAGNETIC FLUCTUATION AMPLITUDE

The toroidal magnetic field on the equatorial plane outside the vacuum vessel but inside the thick shell is measured using two arrays of B_t sensing coils which consist of 32 outboard and 32 inboard coils,¹⁶ so that a maximum toroidal

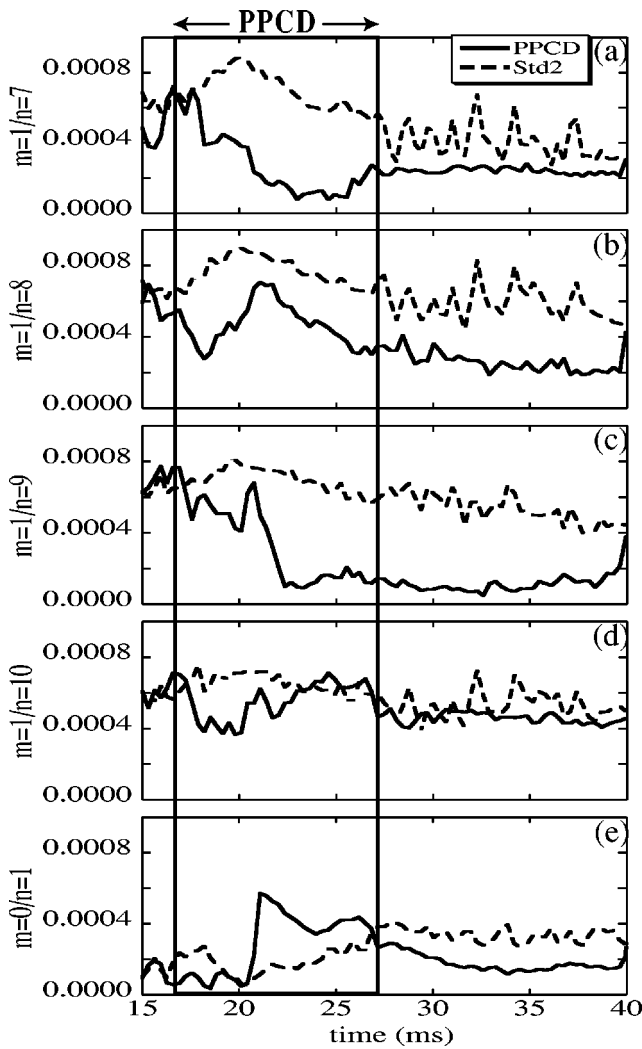


FIG. 3. The amplitudes of the $m=1/n=7$ (a), 8 (b), 9 (c), 10 (d), and $m=0/n=1$ (e) for PPCD (solid line) and Std2 (dashed line) plasmas.

mode number, n , of 16 can be resolved for even ($m=0$) and odd ($m=1$) modes, where m is the poloidal mode number.

Typical amplitudes of the $m=1/n=7-10$ and $m=0/n=1$ modes are compared between PPCD and Std2 in Fig. 3. These modes are all resonant. The $m=1$ mode amplitudes are generally smaller in PPCD than those in Std2. The mode amplitude in PPCD starts to deviate from the levels in Std2 immediately after the first PPCD pulse at $t=17$ ms. The mode amplitude of $m=1/n=7$ in PPCD is 20% of that in Std2 at $t=25$ ms. The mode amplitudes of $m=1/n=8$ and 9, in particular, remain smaller than those in Std2 after the PPCD period. Note that the mode spectrum can change with different F and Θ values [Figs. 1(e) and 1(f)]. The root-mean-square (rms) value of the mode amplitude of $m=1/n=7-10$ at $t=25$ ms in PPCD is 60% of that of Std2. On the other hand, $m=0$ mode amplitudes are comparable to or slightly larger in PPCD than those in Std2 [Fig. 3(e)]. At the moment, we do not understand the reason why the $m=0$ mode increases in PPCD.⁵

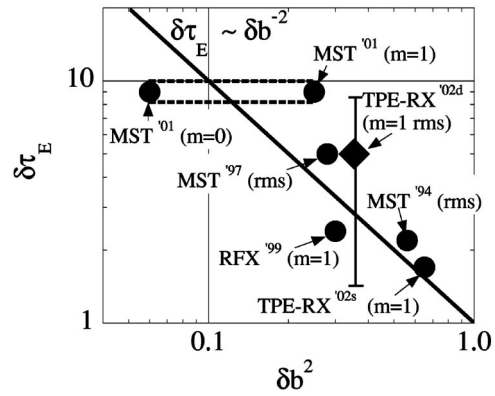


FIG. 4. An increment of energy confinement time, $\delta\tau_E$, is plotted for the present work (diamond) with the standard deviation and for previous works (circles), as a function of δb^2 , which is the square of PPCD magnetic field fluctuation amplitude normalized by that in the case without PPCD. The solid line shows a reference line of $\delta\tau_E \sim \delta b^{-2}$.

V. DISCUSSION

In this section, we compare the increment of τ_E with that in the previous PPCD experiments^{3-6,8} in terms of the magnetic fluctuation amplitude and a parameter reflecting the RFP configuration.¹¹

Five PPCD experiments^{3-6,8} have been reported, and we can add the present work to the PPCD database. First, the factor by which τ_E increases, $\delta\tau_E$, is plotted versus δb^2 , which is the square of the magnetic fluctuation amplitude in PPCD normalized by that in the case without PPCD (Fig. 4). Note that δb^2 is calculated from the available magnetic fluctuation signals in Refs. 3-6,8 at the time when $\delta\tau_E$ is maximum during the PPCD period. The information of the mode number or the rms value in calculating δb^2 is shown in Fig. 4. Previous results are plotted with black circles, and the present work is represented by a diamond. The solid line corresponds to $\delta\tau_E \sim \delta b^{-2}$, which is predicted based on the theory of the transport in a stochastic magnetic field.¹⁷ We have pointed out⁸ that the previous PPCD results seem to follow this reference line. Figure 4 shows that a fivefold improvement of τ_E in the present work is located off the reference line if the rms value is used for δb^2 . We also note in Fig. 4 that the data points of $\delta\tau_E$ using the $m=1$ mode amplitude tend to rise more steeply than the reference line, which indicates that the transport in the highly improved PPCD experiments ($\delta\tau_E > 5$) may be by a mechanism different from the stochasticity of the magnetic field line. Strong magnetic shear in the PPCD operation can reduce the pressure-driven instability, for example.

Another comparison of $\delta\tau_E$ is made in terms of a parameter reflecting the RFP configuration as a function of F and Θ . In RFP plasmas, F and Θ tend to follow a line of constant $\gamma [(1-F)/\Theta]$ when B_{ta} is varied shot by shot.¹⁸ On the other hand, in the PPCD experiments, we noted that γ increases in time during the PPCD period.⁸ Note, in the range of F and Θ explored in the present work, γ is approximately a linear function of (I_θ/I_p) , where I_θ is the total poloidal plasma current flowing between the magnetic axis and the plasma surface. Figure 5(a) shows shot-averaged temporal

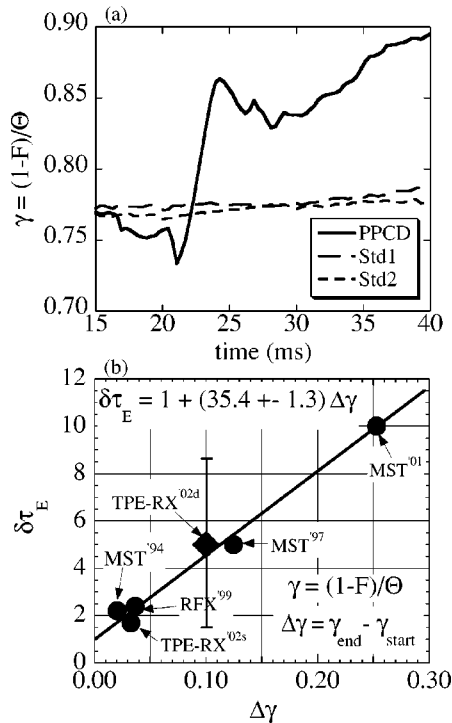


FIG. 5. Shot-averaged temporal evolution of $\gamma [(1-F)/\Theta]$ (a) for PPCD (solid line, diamond), Std1 (long-dashed line, square) and Std2 (dashed line, triangle) in a time period of $t=15\text{--}40$ ms. An increment of energy confinement time, $\delta\tau_E$, is plotted (b) for the present work (diamond) and for the previous works (circles), as a function of $\Delta\gamma$ which is the difference of $\gamma [(1-F)/\Theta]$ between the start and the end, or the time when τ_E is evaluated, in the PPCD period.

evolutions of γ in PPCD, Std1 and Std2. Figure 5(a) shows that γ initially decreases slightly after the first PPCD pulse, then rapidly increases after the second PPCD pulse, and becomes saturated at $t\sim 25$ ms, when τ_E has a peak [Fig. 2(f)], which may indicate that reduced transport is related to γ . The amount ($\Delta\gamma$) by which γ changes between $t\sim 17$ ms and 25 ms is approximately 0.1. It was shown in Ref. 11 that $\delta\tau_E$ linearly increases with $\Delta\gamma$, and that $\Delta\gamma$, which is an indicator of the driven poloidal current, can be a simple figure of merit for PPCD. The improvement in the present work is plotted with the previous results as a function of $\Delta\gamma$ in Fig. 5(b). Although the standard deviation of $\delta\tau_E$ is large, $\delta\tau_E$ in the present work is not contradictory to the overall linear trend. The best fit for the six data points yields $\delta\tau_E=1+35\Delta\gamma$. This apparent strong correlation indicates importance of the increase of I_θ for confinement improvement in RFP plasmas.

VI. SUMMARY AND CONCLUSIONS

The results of the upgraded PPCD experiment in the TPE-RX RFP device were presented. The energy of the main toroidal reversal bank was increased, and an additional toroidal field coil system was installed so that the double-pulse PPCD operation was possible. This has allowed better performance than in the first single-pulse PPCD experiment in TPE-RX.⁸ The result for the new PPCD was compared with those of two kinds of standard discharge, Std1 and Std2 at $I_p\sim 350$ kA. It was shown that all of the measured thermal

properties, n_{el} , T_{e0} , and T_i , increased from those in Std1 and Std2. The global confinement properties β_p and τ_E were calculated assuming fixed shape of spatial profiles including finite dW_s/dt and using the $\alpha\text{-}\Theta\Theta$ model. On average, the results showed a twofold improvement in β_p and fivefold improvement in τ_E , which is similar to the improvement reported earlier in MST.⁴ Magnetic field fluctuation amplitudes were also compared, using B_t signals. The square of the rms amplitude of $m=1$ modes became 36% of those in Std1 and Std2. The increment of τ_E , $\delta\tau_E$, was discussed in terms of δb^2 and $\Delta\gamma$ in comparison with the results of previous PPCD experiments.^{3–6,8} It was shown that $\delta\tau_E$ is approximately consistent with the overall tendency shown in the previous PPCD database. In particular, it was shown here that $\Delta\gamma$ can be a figure of merit for PPCD.

ACKNOWLEDGMENTS

The authors are grateful to Dr. Y. Owadano for his encouragement and support of this work. This work was financially supported by the Budget for Nuclear Research of the Ministry of Education, Culture, Sports, Science and Technology based on screening and counseling by the Atomic Energy Commission.

- ¹H. A. B. Bodin and A. A. Newton, Nucl. Fusion **20**, 1255 (1980).
- ²H. K. Moffat, in *Magnetic Field Generation in Electrically Conducting Fluids* (Cambridge University Press, Cambridge, 1978).
- ³J. S. Sarff, S. A. Hokin, H. Ji, S. C. Prager, and C. R. Sovinec, Phys. Rev. Lett. **72**, 3670 (1994).
- ⁴J. S. Sarff, N. E. Lanier, S. C. Prager, and M. R. Stoneking, Phys. Rev. Lett. **78**, 62 (1997).
- ⁵B. E. Chapman, J. K. Anderson, T. M. Biewer, D. L. Brower, S. Castillo, P. K. Chattopadhyay, C.-S. Chiang, D. Craig, D. J. Den Hartog, G. Fiksel, P. W. Fontana, C. B. Forest, S. Gerhardt, A. K. Hansen, D. Holly, Y. Jiang, N. E. Lanier, S. C. Prager, J. C. Reardon, and J. W. Warff, Phys. Rev. Lett. **87**, 205001 (2001).
- ⁶R. Bartiromo, P. Martin, S. Martini, T. Bolzonella, A. Canton, P. Innocente, L. Marrelli, A. Murari, and R. Pasquarotto, Phys. Rev. Lett. **82**, 1462 (1999).
- ⁷Y. Yagi, S. Sekine, H. Sakakita, H. Koguchi, K. Hayase, Y. Hirano, I. Hirota, S. Kiyama, Y. Maejima, Y. Sato, T. Shimada, and K. Sugisaki, Fusion Eng. Des. **45**, 409 (1999).
- ⁸Y. Yagi, Y. Maejima, H. Sakakita, Y. Hirano, H. Koguchi, T. Shimada, and S. Sekine, Plasma Phys. Controlled Fusion **44**, 335 (2002).
- ⁹B. E. Chapman, A. F. Almagri, J. K. Anderson, C.-S. Chiang, D. Craig, G. Fiksel, N. E. Lanier, S. C. Prager, J. S. Sarff, M. R. Stoneking, and P. W. Terry, Phys. Plasmas **5**, 1848 (1998).
- ¹⁰N. E. Lanier, D. Craig, J. K. Anderson, T. M. Biewer, B. E. Chapman, D. J. Den Hartog, C. B. Forest, S. C. Prager, D. L. Brower, and Y. Jiang, Phys. Rev. Lett. **85**, 2120 (2000).
- ¹¹Y. Yagi, H. Koguchi, Y. Hirano, H. Sakakita, T. Shimada, and S. Sekine, J. Phys. Soc. Jpn. **71**, 2574 (2002).
- ¹²B. E. Chapman, A. F. Almagri, J. K. Anderson, T. M. Biewer, P. K. Chattopadhyay, C.-S. Chiang, D. Craig, D. J. Den Hartog, G. Fiksel, C. B. Forest, A. K. Hansen, D. Holly, N. E. Lanier, R. O'Connell, S. C. Prager, J. C. Reardon, J. S. Sarff, M. D. Wyman, D. L. Brower, W. X. Ding, Y. Jiang, S. D. Terry, P. Franz, L. Marrelli, and P. Martin, Phys. Plasmas **9**, 2061 (2002).
- ¹³Y. Yagi, Nucl. Fusion **40**, 1933 (2000).
- ¹⁴K. Miyamoto, N. Asakura, A. Ejiri, A. Fujisawa, T. Fujita, N. Inoue, H. Ji, S. Matsui, K. Mayanagi, J. Morikawa, H. Morimoto, D. Nagahara, Y.

- Nagayama, H. Nihei, S. Ohdachi, T. Okabe, Y. Shimazu, K. Shimoji, S. Shinohara, A. Shirai, S. Takeji, H. Toyama, K. Yamagishi, and Z. Yoshida, *Proceedings of Invited Papers*, 13th International Conference on Plasma Physics and Controlled Fusion Research, Washington, 1990 (IAEA, Vienna, 1991), Vol. 2, p. 525.
- ¹⁵V. Antoni, D. Merlin, S. Ortolani, and R. Paccagnella, *Nucl. Fusion* **26**, 1711 (1986).
- ¹⁶Y. Yagi, H. Sakakita, S. Sekine, H. Koguchi, S. Kiyama, and T. Osakabe, *Fusion Eng. Des.* **46**, 47 (1999).
- ¹⁷A. B. Rechester and M. N. Rosenbluth, *Phys. Rev. Lett.* **40**, 38 (1978).
- ¹⁸S. Martini, D. Terranova, P. Innocente, and T. Bolzonenlla, *Plasma Phys. Controlled Fusion* **41**, A315 (1999).